Eur Biophys J (2011) 40:1237–1245
DOI 10.1007/s00249-011-0736-x

ORIGINAL PAPER

EBSA
Biophysics in Europe

Protein structural changes induced by glutathione-coated CdS quantum dots as revealed by Trp phosphorescence

E. Gabellieri · P. Cioni · E. Balestreri · E. Morelli

Received: 4 March 2011 / Revised: 24 June 2011 / Accepted: 30 June 2011 / Published online: 13 July 2011
© European Biophysical Societies' Association 2011

Abstract We evaluated the potential of tryptophan (Trp) phosphorescence spectroscopy for investigating conformational states of proteins involved in interaction with nanoparticles. Characterization of protein–nanoparticle interaction is crucial in assessing biological hazards related to use of nanoparticles. We synthesized glutathione-coated CdS quantum dots (GSH-CdS), which exhibited an absorption peak at 366 nm, indicative of 2.4 nm core size. Chemical analysis of purified GSH-CdS suggested an average molecular formula of $GSH_{18}S_{56}Cd_{60}$. Investigations were conducted on model proteins varying in terms of isoelectric point, degree of burial of the Trp probe, and quaternary structure. GSH-CdS fluorescence measurements showed improvement in nanoparticle quantum yield induced by protein interaction. Trp phosphorescence was used to examine the possible perturbations in the protein native fold induced by GSH-CdS. Phosphorescence lifetime measurements highlighted significant conformational changes in some proteins. Despite their small size, GSH-CdS appeared to interact with more than one protein molecule. Rough determination of the affinity of GSH-CdS for proteins was derived from the change in phosphorescence lifetime at increasing nanoparticle concentrations. The estimated affinities were comparable to those observed for specific protein–ligand interactions and suggest that protein–nanoparticle interaction may have a biological impact.

Special Issue: SIBPA 2011 Meeting.

E. Gabellieri (✉) · P. Cioni · E. Balestreri · E. Morelli
Institute of Biophysics, via G. Moruzzi, 1, 56124 Pisa, Italy
e-mail: edi.gabellieri@pi.ibf.cnr.it

Keywords Glutathione-coated CdS quantum dots · Protein–nanoparticle interaction · Room-temperature phosphorescence · Fluorescence of nanoparticles

Introduction

The advent of nanotechnologies has had a major impact on a wide range of medical and biological applications, as well as electronics, water treatment technologies, and solar cells (Brown and Kamat 2008; Bruchez et al. 1998; Deliyanni et al. 2003; Michalet et al. 2005; Wu et al. 2003). Progress in these fields, however, has raised concerns about human health and environmental hazards. There is some evidence of toxicity of nanoparticles to bacteria, algae, aquatic invertebrates, fish species, and mammalian cell cultures (Handy et al. 2008). However, little is known about how such systems are affected, and safety remains an open issue. Since the biological effect at cellular level is the sum of interactions at molecular level, studying the interaction of nanoparticles with biomolecules may be the key factor for understanding the uptake and toxicity mechanisms in living organisms. Proteins are fundamental for the proper functioning of cells and organisms, thus the impact of nanoparticles on living organisms in terms of protein structural changes is a critical issue that has attracted increasing attention (Deng et al. 2011).

In a biological environment, nanoparticles are immediately covered by a corona of rapidly exchanged biomolecules, consisting mainly of proteins (Hellstrand et al. 2009; Lundqvist et al. 2008). The protein coating changes the chemical nature of the particle surface and consequently can influence its fate in the body, by promoting or obstructing uptake by cells (Lynch et al. 2007, 2009). Interaction with nanoparticles may result in loss of protein structure,

leading to loss of biological activity (Hong et al. 2004; Lundqvist et al. 2004; Shang et al. 2007). Moreover, the conformational changes induced in the protein by nanoparticle interaction may in turn affect biological mechanisms (Deng et al. 2011).

Several different nanoparticle and protein combinations have recently been studied using different techniques, such as size-exclusion chromatography, isothermal titration calorimetry, circular dichroism, fluorescence, and Fourier-transform infrared spectroscopy (Cedervall et al. 2007; De et al. 2007; Jiang et al. 2010; Rocker et al. 2009; Sabatino et al. 2007). So far, the results show that the interaction is dependent on specific protein–nanoparticle pairs, and there are many open issues regarding the general paradigms (Lynch and Dawson 2008). In addition, the analysis of more recent results highlights the importance of investigating the microscopic details of the corona (Monopoli et al. 2011).

Semiconductor nanoparticles, also termed quantum dots (QDs), such as CdS, CdSe and CdTe, have been extensively studied, due to their size-tunable optical, electronic, and catalytic properties (Alivisatos et al. 1996; Michalet et al. 2005). QDs in the range of 2–6 nm are interesting due to their dimensional matching with biomolecules (Medintz et al. 2005) and seem to be very promising agents also for in vivo imaging (Tavares et al. 2011). QDs are typically produced in organic solvents, resulting in hydrophobic nanoparticles which are insoluble in water and not suitable for biomedical purposes. Water-soluble surface stabilizers have been successfully employed to coat QDs, which have then been used as fluorescent probes in a variety of biological applications (Bruchez et al. 1998; Medintz et al. 2005). Of the commonly used coating agents, thiol-containing molecules, such as mercaptoethanol, cysteine, glutathione, and phytochelatins, have been usefully employed for direct synthesis of biocompatible CdS quantum dots (Bae and Mehra 1998; Jiang et al. 2007; Thangadurai et al. 2008).

In this study, glutathione (GSH) was chosen as a capping ligand of CdS QDs, following a simple procedure at room temperature, which involves directly incorporating sulfide into preformed Cd-GSH complexes (Nguyen et al. 1999). The interaction between glutathione-coated CdS quantum dots (GSH-CdS) and model proteins was studied by fluorescence and Trp phosphorescence spectroscopy. The Trp phosphorescence lifetime (τ) depends on the local viscosity, and increases by 3–4 orders of magnitude from fluid to rigid matrices (Strambini and Gonnelli 1995). In proteins, τ is essentially a monitor of the local flexibility of the protein structure around the phosphorescent Trp residue, and is quickly affected even by minor changes in protein conformation (Gonnelli and Strambini 1995, 2005). Trp phosphorescence has been applied to study even subtle changes in protein conformation such as those induced by ligand binding (Cioni and Strambini 1989; Strambini and Gabellieri 1990), subunit association (Strambini et al. 1989), protein–protein interactions (Gabellieri and Strambini 1994), as well as variations in physical and chemical properties of the solution (Cioni and Strambini 2002; Strambini and Gabellieri 1996). In addition, Trp phosphorescence has been usefully employed for investigating the effect on protein conformational states of adsorption on solid surface (Gabellieri and Strambini 2000, 2001). Trp phosphorescence has also been applied for investigating the interaction of model proteins with dendrimers, synthetic polymers of nanometric size (Gabellieri et al. 2006).

In the current study, model systems were selected from proteins with well-characterized phosphorescence properties in a wide range of experimental conditions, with known crystallographic structure and various degrees of quaternary structure, namely C112S-azurin (C112S-Az) (monomer), liver alcohol dehydrogenase (LADH) (dimer), aldolase (Ald) (tetramer), and glyceraldehyde-3-phosphate dehydrogenase (GAPDH) (tetramer). In the selected proteins, the emission is due entirely to a single Trp residue per subunit, which has been identified in all the above proteins except Ald. In the latter, the emission is from either W295 or W313, or both, as the third residue, W147, is totally quenched by C149, which is in direct contact with it (Gonnelli and Strambini 2005).

Our results highlight that GSH-CdS can interact with proteins, forming complexes in which the protein structure may be significantly altered. The induced conformational changes are not confined to the superficial layers of the protein structure, but seem to propagate to the internal regions where the phosphorescent probes are localized.

Materials and methods

Chemicals and proteins

All reagents were of analytical grade: reduced glutathione (GSH) was from Sigma-Aldrich (St. Luis, MO); $Na_2S{\cdot}9H_2O$, $CdCl_2{\cdot}H_2O$, and tris(hydroxymethyl)aminomethane (Tris) were from Carlo Erba (Milan, Italy). A solution of 50 mM Tris at pH 8 was used throughout the work. Water was purified by a Milli-Q Plus system (Millipore Corporation, MA). Glyceraldehyde-3-phosphate dehydrogenase (GAPDH) from *Bacillus stearothermophilus* was kindly supplied by Prof. G. Branlant, University Henri Poincaré (Nancy, France). The azurin C112S mutant (C112S-Az) was constructed using the Quik Change kit (Stratagene, La Jolla, CA) and confirmed by sequencing. C112S-Az was prepared as described elsewhere (Karlsson et al. 1989). With respect to the native protein, the C112S mutant has lost the ability to bind metal ions. Horse liver

alcohol dehydrogenase (LADH) was a generous gift from Dr M. Gonnelli, Institute of Biophysics (CNR, Pisa, Italy). Rabbit muscle aldolase (Ald) was from Sigma–Aldrich (St. Luis, MO). Before use, a suitable amount of each protein stock was dialyzed overnight against Tris buffer.

Preparation of synthetic GSH-coated CdS quantum dots

In vitro synthesis of GSH-coated CdS quantum dots (GSH-CdS) was performed by following the procedure reported by Nguyen et al. (1999) with some modifications. $CdCl_2$ was added to a solution of 10 mM GSH in 50 mM Tris (pH 8) at GSH:Cd molar ratio of 2, bubbled with nitrogen, and left to react for 10 min. Sodium sulfide was then added to the preformed Cd-GSH complexes at S:Cd molar ratio of 1 under a nitrogen atmosphere, and the sample was incubated at room temperature for 30 min under stirring. By following this procedure, a pale-yellow solution of GSH-CdS was obtained. Finally, the solution was degassed with nitrogen (30 min) to remove excess free sulfide, stored in the dark at +4°C, and used within a few days. Before the reaction with proteins, small sample volumes (500 µl) were dialyzed (cut-off 3,500 Da) overnight against the same Tris buffer to remove unreacted reagents.

Chemical characterization of GSH-CdS

Dialyzed GSH-CdS were assayed for their GSH, Cd, and sulfide contents. GSH was analyzed by pre-column derivatization with monobromobimane (mBrB) by following the procedure reported elsewhere (Morelli and Scarano 2001). The high-performance liquid chromatography (HPLC) system consisted of two Shimadzu LC-10 AD pumps, a Rheodyne 7725 injection valve connected to a 50-µl loop, a RF–10 AXL Shimadzu fluorescence detector, and a Kinetex (Phenomenex) 2.6 µm C18 reverse-phase column (100 × 4.6 mm). A linear gradient from 10% to 12% acetonitrile in water containing 0.1% trifluoroacetic acid for 7 min was used at flow rate of 1 ml min^{-1}.

Cd determination was carried out by atomic absorption spectroscopy using a PerkinElmer spectrophotometer (model 1100 B) equipped with a graphite furnace (model HGA 700).

Acid-labile sulfide (S) was determined by the methylene blue method (Rabinowitz 1978), by following the procedure reported elsewhere (Scarano and Morelli 2003).

Spectroscopic measurements

Absorption spectra were measured by a double-beam JASCO V-550 UV/Vis spectrophotometer. Fluorescence measurements were performed using a Fluoromax-4 spectrofluorometer. Emission spectra were recorded using an excitation wavelength of 366 nm. Blank spectra, recorded under the same conditions, were subtracted throughout.

Phosphorescence decays were measured with pulsed excitation on a home-made apparatus (Strambini et al. 2004). The exciting light (λ_{ex} = 292 nm) was provided by a frequency-doubled Nd:YAG-pumped dye laser (Quanta Systems, Milan, Italy) with pulse duration of 5 ns and typical energy per pulse around 0.05 mJ. Phosphorescence intensity was collected at 90° from the vertical excitation through a filter combination with a transmission window of 405–445 nm (WG405; Lot-Oriel, Milan, Italy, plus interference filter DT-Blau; Balzer, Milan, Italy) and monitored by a photomultiplier (EMI 9235QA, Middlesex, UK). The prompt Trp fluorescence intensity from the same pulse was used to account for possible variations in the laser output between measurements, as well as to obtain fluorescence-normalized phosphorescence intensities. All phosphorescence decays were analyzed in terms of discrete exponential components by a nonlinear least-squares fitting algorithm (DAS6 fluorescence decay analysis software; Horiba Jobin–Yvon, Milan, Italy).

Results and discussion

Characterization of GSH-CdS

GSH-coated CdS quantum dots were synthesized in vitro by incorporating sulfide into preformed GSH-Cd complexes at GSH:Cd:S stoichiometric ratio of 2:1:1, as described in the experimental section. Optical and chemical properties of GSH-CdS are shown in Fig. 1 and Table 1. The absorption spectrum exhibited a narrow peak centered at 366 nm (Fig. 1). As the position of the absorption peak is related to the average size of the CdS core of the nanoparticles (Efros and Rodina 1989), a diameter of 2.4 nm was calculated for the inorganic inner core, according to Yu et al. (2003). Barglik-Chory et al. (2003) assessed the thickness of the GSH capping around the CdS inner core to be 0.5 nm. Using this value, we estimated the overall size of the synthesized nanoparticles as being approximately 3.4 nm. The concentration of GSH-CdS was determined from the absorbance at 366 nm, by using the ε value calculated from Yu's equation (Yu et al. 2003), as reported in Table 1. Chemical assays of the synthesized GSH-CdS showed a Cd:S:GSH molar ratio close to 1:0.9:0.3. A similar S:Cd ratio (0.92) was also determined by Thangadurai et al. (2008), in a structural and photophysical study carried out on thiol-capped CdS. By taking into account the ratio between the concentrations of GSH, Cd, S, and GSH-CdS, we inferred an average molecular formula of $GSH_{18}S_{56}Cd_{60}$. This formula is in rough agreement with the

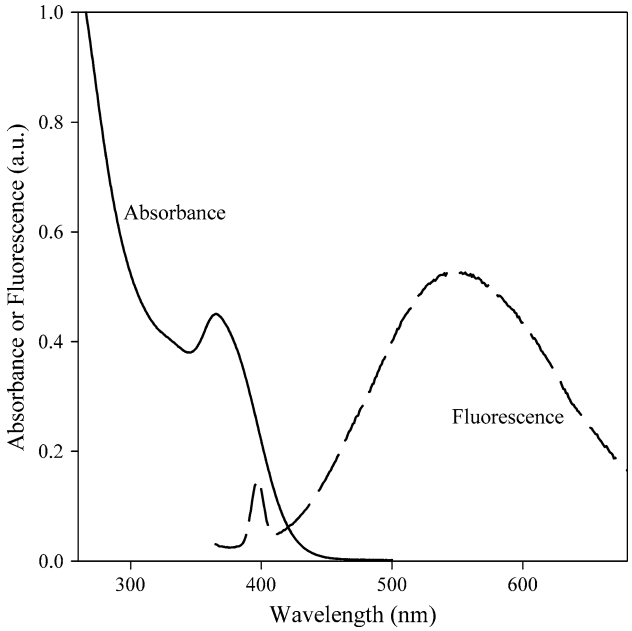

Fig. 1 Absorption spectrum (*solid line*) and fluorescence emission spectrum (*dashed line*) of GSH-CdS in 50 mM Tris, pH 8 at 20°C; excitation wavelength, 366 nm

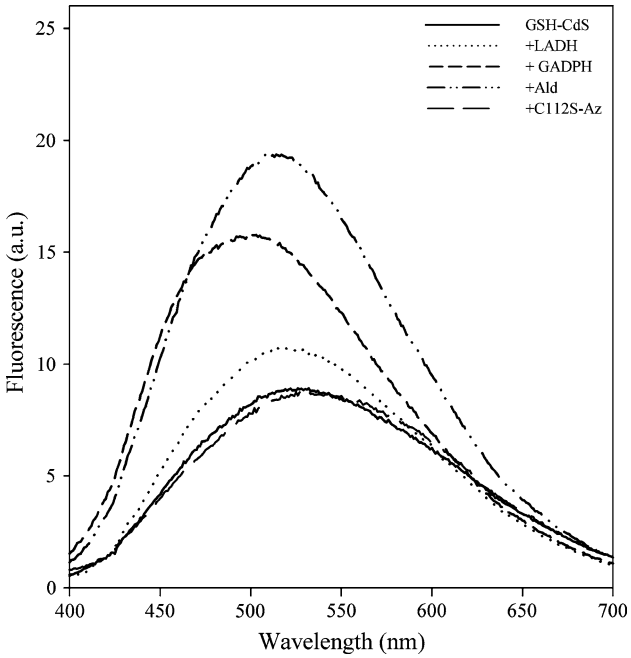

Fig. 2 Fluorescence emission spectra of a 0.8 μM GSH-CdS solution before and after addition of C112S-Az, LADH, GAPDH or Ald at final concentration of 2 μM in 50 mM Tris, pH 8

inorganic core of 70–90 atoms of Cd described by other authors for GSH-CdS (Neder and Korsunskiy 2005).

The fluorescence emission spectrum ($\lambda_{ex} = 366$ nm) shows a large Stokes shift, with the maximum of the emission located at 530 nm (Fig. 1). The spectrum shape appears rather broad (~175 nm, half-band width), as often described for CdS nanoparticles synthesized in aqueous solution (Chestnoy et al. 1986; Zou et al. 2009). Overall, the optical properties agree well with those reported by other authors using different protocols for nanoparticle synthesis (Barglik-Chory et al. 2003; Jiang et al. 2007; Zou et al. 2009).

Effect of model proteins on the fluorescence emission of GSH-CdS

Addition of micromolar quantities of different proteins changed the fluorescence properties of GSH-CdS. Figure 2 shows that 2 μM Ald, GAPDH, and LADH shifted the peak wavelength and increased the fluorescence intensity of 0.8 μM GSH-CdS. Table 2 summarizes the changes induced in the fluorescence emission of the nanoparticles by each protein. A blue-shift in the peak wavelength of 22 and 30 nm induced by Ald and GAPDH, respectively, was measured. Ald and GAPDH also produced a remarkable effect on the quantum yield of GSH-CdS, which increased 1.9 and 1.6 times, respectively. A smaller but significant enhancement in the fluorescence intensity was also induced by LADH. The emission properties of QDs mainly depend on the surface structure, especially surface defects (Spanhel et al. 1987). Consequently, changes in quantum yield of fluorescence are directly related to changes in the surface states. These changes may be induced by different coating agents (Thangadurai et al. 2008), or the formation of complexes between ions and surface groups (Chen and Rosenzweig 2002), or protein binding (Jiang et al. 2007).

Based on this evidence, the increase in fluorescence emission observed in our experimental conditions suggests that LADH, Ald, and GAPDH interact with GSH-CdS strongly enough to alter the states distribution on the surface of the nanoparticles. On the other hand, no effect on the spectrum and quantum yield of QDs was measured after addition of C112S-Az up to 10 μM. This finding indicates the absence of any interaction between C112S-Az and GSH-CdS. The different behavior of the examined proteins

Table 1 Chemical properties of dialyzed GSH-CdS

λ_{max}	Diameter[a] (nm)	ε_M[a]	[GSH-CdS] μM	[GSH] μM	[S] μM	[Cd] μM
366	2.4	1.65×10^5	50	905 ± 180	2,800 ± 300	3,000 ± 200

[a] Calculated from equations in Yu et al. (2003)

Table 2 Fluorescence emission properties of GSH-CdS before and after protein addition

Sample	Peak (nm)	Half-band width (nm)	Relative quantum yield[a]
GSH-CdS	530	177	1.0
GSH-CdS + LADH	518	160	1.1
GSH-CdS + Ald	508	151	1.9
GSH-CdS + GAPDH	500	154	1.6

[a] Fluorescence quantum yield was calculated by integration of the emission spectrum of samples at the same absorbance. Relative quantum yield is the ratio between the fluorescence emission of GSH-CdS with added protein and that of GSH-CdS alone

suggests that the interaction of GSH-CdS is not common to all proteins but rather depends on specific molecular characteristics. In our experimental conditions, at pH 8, nanoparticles covered by residues of glutamic acid of GSH were negatively charged. At this pH, C112S-Az is negative (pI 5.4), while LADH, GAPDH, and Ald are positive (pI 8.3, 8.44, and 8.2, respectively), and for these three proteins, it is reasonable to suppose that the interaction with GSH-CdS is facilitated. Although the number of proteins examined here was limited, the correlation between protein charge and binding to GSH-CdS seems to indicate the importance of electrostatic attraction for this interaction. Electrostatic attraction has often been indicated as the main force governing surface adsorption of protein, using both experimental approaches and molecular dynamics simulation (Arai and Norde 1990; Hung et al. 2011; Makarucha et al. 2011).

Effect of GSH-CdS on the phosphorescence lifetime of model proteins

Phosphorescence spectroscopy was applied to investigate the possible protein conformational changes induced by the interaction with GSH-CdS. The effect of GSH-CdS (10 μM) on the phosphorescence lifetime of the model proteins (1–3 μM) was measured at 20°C in 50 mM Tris, pH 8. Figure 3 shows the decay in phosphorescence intensity of GAPDH after addition of GSH-CdS. The reduction in the signal-to-noise ratio, observed in the presence of GSH-CdS, was mainly due to its absorbance at the excitation wavelength. No signal from GSH-CdS was measured in the wavelength range of the Trp phosphorescence emission. The inner filter effect did not affect the decay rate. With the exception of C112S-Az, whose emission decays exponentially, the phosphorescence decay of each protein is not exponential, both before and after addition of QDs. Consequently, we decided to analyze the decay data in terms of the average lifetime, τ ($\tau = \Sigma\alpha_i\tau_i$, where α_i is the amplitude of the τ_i component) obtained by a two-component fit to the decay. Multiple lifetime components arise from the

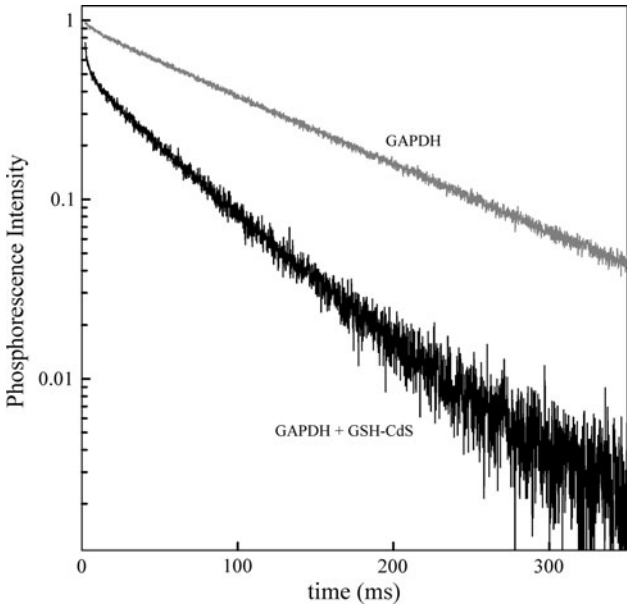

Fig. 3 Comparison between Trp phosphorescence decay of GAPDH (1.3 μM) before and after addition of GSH-CdS (10 μM), in 50 mM Tris, pH 8 at 20°C. The triplet-state lifetimes, τ_i, and the pre-exponential terms, α_i, obtained from a two-component fit to the phosphorescence decay [$P(t) = \alpha_1 e^{-t/\tau 1} + \alpha_2 e^{-t/\tau 2}$] are $\tau_1 = 9$ ms ($\alpha_1 = 0.09$) and $\tau_2 = 113$ ms ($\alpha_2 = 0.91$) for GAPDH alone and $\tau_1 = 3$ ms ($\alpha_1 = 0.50$) and $\tau_2 = 55$ ms ($\alpha_2 = 0.50$) for GAPDH + GSH-CdS

conformational heterogeneity of protein in solution (Cioni et al. 1994), a heterogeneity that is apparently increased in the presence of QDs (Fig. 3). For each protein, Table 3 reports the Trp residue responsible for the phosphorescence emission and its minimum distance from the solvent interface (r_p), as measured from the crystallographic structures. Table 3 also shows the Trp intrinsic phosphorescence lifetime (τ_0), and the change in τ induced by GSH-CdS, as measured by the lifetime ratio (τ/τ_0). The τ/τ_0 values reveal that the phosphorescence lifetime of LADH, GAPDH, and Ald was significantly altered by GSH-CdS, whereas that of C112S-Az was unchanged. This finding thus shows the same trend as the QD fluorescence measurements. The increase in QD fluorescence intensity induced by LADH, Ald, and GAPDH is concomitant with changes in their conformational states, as highlighted by the decrease in the phosphorescence lifetime. On the other hand, the inability of C112S-Az to affect the fluorescence properties of GSH-CdS is in agreement with no change in lifetime.

Trp phosphorescence lifetime is a monitor of the internal flexibility in proteins. A decrease in τ indicates an increase in the internal mobility of the protein structure (Gonnelli and Strambini 1995, 2005). In the case of LADH, GAPDH, and Ald, QDs cause a reduction in τ as if, locally, the native fold becomes more flexible through its association with

Table 3 Change in phosphorescence lifetime (τ) of different proteins after addition of 10 μM GSH-CdS in 50 mM Tris, pH 8, at 20°C

Protein	Trp[a]	r_p[b] (Å)	τ_0[c] (ms)	τ/τ_0
C112S-Az	W48	8.0	340 ± 20	1.00
GAPDH	W84	5.5	98 ± 10	0.53
LADH	W314	4.5	450 ± 25	0.75
Ald	W313/W295	3–4	20 ± 2	0.67

[a] Residue responsible for the phosphorescence emission at room temperature

[b] Thickness of the protein spacer separating the indole ring from the solvent interface, measured from crystallographic structures

[c] Trp intrinsic phosphorescence lifetime

them. The effects of the interaction propagate to the interior of the macromolecule (3–5.5 Å, see Table 3) and alter the environment around the phosphorescent residue. On the other hand, for the deepest Trp residue, W48 of C112S-Az, our results show that the structure within the internal rigid core (r_p = 8 Å) is unaffected by GSH-CdS. Thus, a possible perturbation of protein flexibility in the outer layer, if any, does not propagate to the interior.

A decrease in τ may also be caused by quenching reactions with the chemical groups of the nanoparticle itself or with traces of unreacted reagents. Caution is particularly necessary with GSH-CdS because sulfur compounds, such as sulfhydryl and disulfide groups, are strong quenchers of Trp phosphorescence (Bent and Hayon 1975; Lapidus et al. 2001). We checked to ensure that the GSH-Cd complex (before sulfide addition) did not affect the decay rate of Trp. In GSH-CdS, S^{2-} ions are thought to be bound to Cd^{2+} to form the inner crystalline core, and the thiol group of GSH is involved in the binding of Cd of the external layer. Consequently, sulfur groups should not be available for quenching. To definitively rule out quenching effects we carried out the phosphorescence lifetime measurements at increasing concentrations of GSH-CdS. In fact, a nonlinear dependence of the decay rate ($1/\tau$) on the perturbing agent concentration is a strong indication that quenching mechanisms are not dominant. The nonlinear behavior of $1/\tau$ versus [GSH-CdS] observed for LADH, Ald, and GAPDH (Fig. 4) reasonably rules out strong quenching effects, at least in our experimental conditions.

For each protein, the curve was roughly hyperbolic, reminiscent of a binding curve. Two kinds of parameters may be estimated from the profiles of Fig. 4. First, we can evaluate the dissociation constant of the complex (K_D). In fact, in a binding process of a phosphorescent protein to an non-phosphorescent ligand, the overall decay rate ($1/\tau$) depends on the decay rates of the free and bound protein and on the equilibrium constant of the reaction, i.e., K_D (Gabellieri and Strambini 1994). The profiles shown in Fig. 4 provide K_D

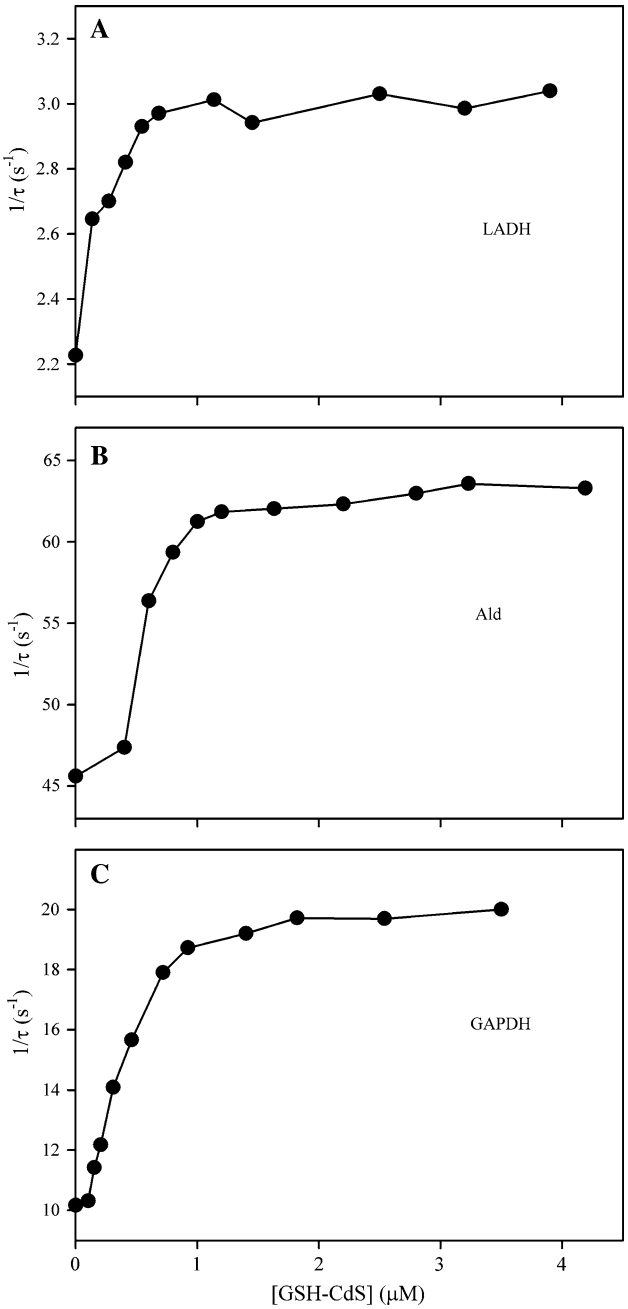

Fig. 4 Effect of GSH-CdS concentration on the phosphorescence lifetime of: **a** 3.1 μM LADH, **b** 3.2 μM Ald or **c** 1.3 μM GAPDH in 50 mM Tris, pH 8 at 20°C

values lower than 0.5 μM for all the proteins measured. This value is similar to those reported for specific protein–ligand complexes, such as subunit–subunit interaction in multimeric proteins (Chothia and Janin 1975), and suggests that the protein–nanoparticle binding may interfere with biological processes. Second, we can evaluate the number of protein molecules bound to one nanoparticle. All curves reach a saturation plateau at protein:QD ratio greater than 1:1 (1.3, 2, and 4.4 saturation ratio was found for GAPDH,

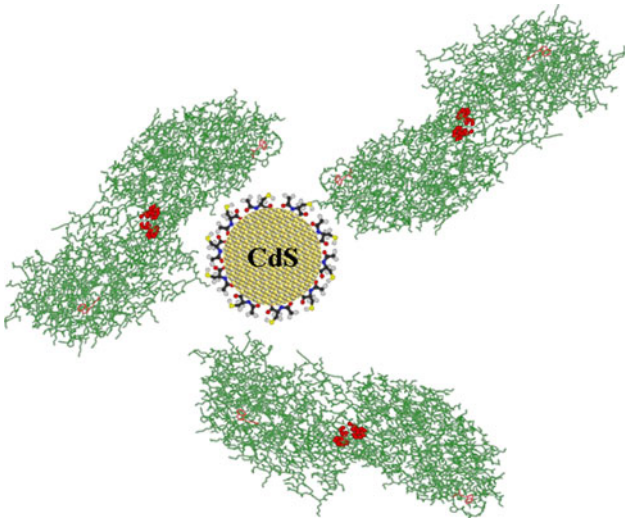

Fig. 5 Schematic depiction of the interaction between proteins and GSH-CdS. Proteins are represented by the crystallographic structure of LADH, in which *bold red spheres* represent phosphorescent Trp

Ald, and LADH, respectively), suggesting that more than one protein molecule binds to one QD. Figure 5 shows the hypothesized interaction between protein and nanoparticle. In their discussion of the energy involved in protein–protein interactions, Chothia and Janin (1975) estimated that an energetically stable complex needs a contact surface area of at least 6 nm^2 (Chothia and Janin 1975). Considering the size of GSH-CdS (3.4 nm overall diameter), the nanoparticle surface area (about 36 nm^2) appears sufficient to yield a stable interaction with a maximum of six protein molecules. Steric hindrance and group-specific repulsion can reduce the number of molecules involved.

Conclusions

We have described the interactions of in vitro-synthesized water-soluble GSH-CdS with selected proteins, by following changes in the fluorescence properties of nanoparticles and in the Trp phosphorescence of proteins. The interaction between some proteins, namely GAPDH, LADH, and Ald, and nanoparticles is proven by the increase in the fluorescence emission of GSH-CdS and the decrease of the protein phosphorescence lifetime. No change in fluorescence and phosphorescence signals was measured in the presence of C112S-Az, suggesting that the interaction is protein dependent. The sensitivity of Trp phosphorescence to perturbations of the native fold showed that the interaction with GSH-CdS may significantly alter the protein structure. The results obtained with model proteins indicated that these conformational changes can propagate to the interior of the macromolecules and loosen the structure. To the best of our knowledge, this is the first time that alterations in the internal dynamics of protein have been detected for this kind of protein–nanoparticle interaction. Protein interaction seems to involve multiple sites on the GSH-CdS surface, in agreement with the protein "corona" model. The estimated affinity was similar to that involved in many protein–ligand complexes, thus supporting the hypothesis of possible effects of nanoparticles on biological processes.

The use of Trp phosphorescence provides a new and interesting approach for understanding the impact of nanoparticles on protein dynamical structure. More in-depth investigations are needed to understand the relationship between conformational and functional changes.

Acknowledgments The technical assistance of Alessandro Puntoni is duly acknowledged.

References

Alivisatos AP, Johnsson KP, Peng X, Wilson TE, Loweth CJ, Bruchez MP Jr, Schultz PG (1996) Organization of 'nanocrystal molecules' using DNA. Nature 382:609–611

Arai T, Norde W (1990) The behavior of some model proteins at solid liquid interfaces. 2. Sequential and competitive adsorption. Colloids Surf 51:17–28

Bae W, Mehra RK (1998) Properties of glutathione- and phytochelatin-capped CdS bionanocrystallites. J Inorg Biochem 69:33–43

Barglik-Chory C, Buchold D, Schmitt M, Kiefer W, Heske C, Kumpf C, Fuchs O, Weinhardt L, Stahl A, Umbach E, Lentze M, Geurts J, Muller G (2003) Synthesis, structure and spectroscopic characterization of water-soluble CdS nanoparticles. Chem Phys Lett 379:443–451

Bent DV, Hayon E (1975) Excited state chemistry of aromatic amino acids and related peptides. III. Tryptophan. J Am Chem Soc 97:2612–2619

Brown P, Kamat PV (2008) Quantum dot solar cells. Electrophoretic deposition of CdSe-C60 composite films and capture of photogenerated electrons with nC60 cluster shell. J Am Chem Soc 130:8890–8891

Bruchez M Jr, Moronne M, Gin P, Weiss S, Alivisatos AP (1998) Semiconductor nanocrystals as fluorescent biological labels. Science 281:2013–2016

Cedervall T, Lynch I, Lindman S, Berggard T, Thulin E, Nilsson H, Dawson KA, Linse S (2007) Understanding the nanoparticle-protein corona using methods to quantify exchange rates and affinities of proteins for nanoparticles. Proc Natl Acad Sci USA 104:2050–2055

Chen Y, Rosenzweig Z (2002) Luminescent CdS quantum dots as selective ion probes. Anal Chem 74:5132–5138

Chestnoy N, Harris TD, Hull R, Brus LE (1986) Luminescence and photophysics of CdS semiconductor clusters: the nature of the emitting electronic state. J Phys Chem 90:3393–3399

Chothia C, Janin J (1975) Principles of protein–protein recognition. Nature 256:705–708

Cioni P, Strambini GB (1989) Dynamical structure of glutamate dehydrogenase as monitored by tryptophan phosphorescence. Signal transmission following binding of allosteric effectors. J Mol Biol 207:237–247

Cioni P, Strambini GB (2002) Effect of heavy water on protein flexibility. Biophys J 82:3246–3253

Cioni P, Gabellieri E, Gonnelli M, Strambini GB (1994) Heterogeneity of protein conformation in solution from the lifetime of tryptophan phosphorescence. Biophys Chem 52:25–34

De M, You CC, Srivastava S, Rotello VM (2007) Biomimetic interactions of proteins with functionalized nanoparticles: a thermodynamic study. J Am Chem Soc 129:10747–10753

Deliyanni EA, Bakoyannakis DN, Zouboulis AI, Matis KA (2003) Sorption of As(V) ions by akaganeite-type nanocrystals. Chemosphere 50:155–163

Deng ZJ, Liang MT, Monteiro M, Toth I, Minchin RF (2011) Nanoparticle-induced unfolding of fibrinogen promotes Mac-1 receptor activation and inflammation. Nat Nanotechnol 6:39–44

Efros AL, Rodina AV (1989) Confined excitons, trions and biexcitons in semiconductor microcrystals. Solid State Commun 72:435708–435715

Gabellieri E, Strambini GB (1994) Conformational changes in proteins induced by dynamic associations. a tryptophan phosphorescence study. Eur J Biochem 221:77–85

Gabellieri E, Strambini GB (2000) Tryptophan phosphorescence as a monitor of protein conformation in molecular films. Biosens Bioelectron 15:483–490

Gabellieri E, Strambini GB (2001) Structural perturbations of azurin deposited on solid matrices as revealed by trp phosphorescence. Biophys J 80:2431–2438

Gabellieri E, Strambini GB, Shcharbin D, Klajnert B, Bryszewska M (2006) Dendrimer-protein interactions studied by tryptophan room temperature phosphorescence. Biochim Biophys Acta 1764:1750–1756

Gonnelli M, Strambini GB (1995) Phosphorescence lifetime of tryptophan in proteins. Biochemistry 34:13847–13857

Gonnelli M, Strambini GB (2005) Intramolecular quenching of tryptophan phosphorescence in short peptides and proteins. Photochem Photobiol 81:614–622

Handy RD, Owen R, Valsami-Jones E (2008) The ecotoxicology of nanoparticles and nanomaterials: current status, knowledge gaps, challenges, and future needs. Ecotoxicology 17:315–325

Hellstrand E, Lynch I, Andersson A, Drakenberg T, Dahlback B, Dawson KA, Linse S, Cedervall T (2009) Complete high-density lipoproteins in nanoparticle corona. Febs J 276:3372–3381

Hong R, Fischer NO, Verma A, Goodman CM, Emrick T, Rotello VM (2004) Control of protein structure and function through surface recognition by tailored nanoparticle scaffolds. J Am Chem Soc 126:739–743

Hung A, Mwenifumbo S, Mager M, Kuna JJ, Stellacci F, Yarovsky I, Stevens MM (2011) Ordering surfaces on the nanoscale: implications for protein adsorption. J Am Chem Soc 133:1438–1450

Jiang C, Xu SK, Yang DZ, Zhang FH, Wang WX (2007) Synthesis of glutathione-capped US quantum dots and preliminary studies on protein detection and cell fluorescence image. Luminescence 22:430–437

Jiang X, Weise S, Hafner M, Rocker C, Zhang F, Parak WJ, Nienhaus GU (2010) Quantitative analysis of the protein corona on FePt nanoparticles formed by transferrin binding. J R Soc Interface 7(suppl 1):S5–S13

Karlsson BG, Pascher T, Nordling M, Arvidsson RH, Lundberg LG (1989) Expression of the blue copper protein azurin from Pseudomonas aeruginosa in Escherichia coli. FEBS Lett 246:211–217

Lapidus LJ, Eaton WA, Hofrichter J (2001) Dynamics of intramolecular contact formation in polypeptides: distance dependence of quenching rates in a room-temperature glass. Phys Rev Lett 87:258101

Lundqvist M, Sethson I, Jonsson BH (2004) Protein adsorption onto silica nanoparticles: conformational changes depend on the particles' curvature and the protein stability. Langmuir 20:10639–10647

Lundqvist M, Stigler J, Elia G, Lynch I, Cedervall T, Dawson KA (2008) Nanoparticle size and surface properties determine the protein corona with possible implications for biological impacts. Proc Natl Acad Sci USA 105:14265–14270

Lynch I, Dawson KA (2008) Protein-nanoparticle interactions. Nano Today 3:40–47

Lynch I, Cedervall T, Lundqvist M, Cabaleiro-Lago C, Linse S, Dawson KA (2007) The nanoparticle-protein complex as a biological entity; a complex fluids and surface science challenge for the 21st century. Adv Colloid Interface Sci 134–135:167–174

Lynch I, Salvati A, Dawson KA (2009) Protein-nanoparticle interactions what does the cell see? Nat Nanotechnol 4:546–547

Makarucha AJ, Todorova N, Yarovsky I (2011) Nanomaterials in biological environment: a review of computer modelling studies. Eur Biophys J 40:103–115

Medintz IL, Uyeda HT, Goldman ER, Mattoussi H (2005) Quantum dot bioconjugates for imaging, labelling and sensing. Nat Mater 4:435–446

Michalet X, Pinaud FF, Bentolila LA, Tsay JM, Doose S, Li JJ, Sundaresan G, Wu AM, Gambhir SS, Weiss S (2005) Quantum dots for live cells, in vivo imaging, and diagnostics. Science 307:538–544

Monopoli MP, Bombelli FB, Dawson KA (2011) Nanoparticle coronas take shape. Nat Nanotechnol 6:11–12

Morelli E, Scarano G (2001) Synthesis and stability of phytochelatins induced by cadmium and lead in the marine diatom Phaeodactylum tricornutum. Mar Environ Res 52:383–395

Neder RB, Korsunskiy VI (2005) Structure of nanoparticles from powder diffraction data using the pair distribution function. J Phys Condens Matter 17:S125–S134

Nguyen L, Kho R, Bae W, Mehra RK (1999) Glutathione as a matrix for the synthesis of CdS nanocrystallites. Chemosphere 38:155–173

Rabinowitz JC (1978) Analysis of acid-labile sulfide and sulfhydryl groups. Methods Enzymol 53:275–277

Rocker C, Potzl M, Zhang F, Parak WJ, Nienhaus GU (2009) A quantitative fluorescence study of protein monolayer formation on colloidal nanoparticles. Nat Nanotechnol 4:577–580

Sabatino P, Casella L, Granata A, Iafisco M, Lesci IG, Monzani E, Roveri N (2007) Synthetic chrysotile nanocrystals as a reference standard to investigate surface-induced serum albumin structural modifications. J Colloid Interface Sci 314:389–397

Scarano G, Morelli E (2003) Properties of phytochelatin-coated CdS nanocrystallites formed in a marine phytoplanktonic alga (Phaeodactylum tricornutum, Bohlin) in response to Cd. Plant Sci 165:803–810

Shang W, Nuffer JH, Dordick JS, Siegel RW (2007) Unfolding of ribonuclease A on silica nanoparticle surfaces. Nano Lett 7:1991–1995

Spanhel L, Haase M, Weller H, Henglein A (1987) Photochemistry of colloidal semiconductors. 20. Surface modification and stability of strong luminescing CdS particles. J Am Chem Soc 109:5649–5655

Strambini GB, Gabellieri E (1990) Temperature-dependence of tryptophan phosphorescence in proteins. Photochem Photobiol 51:643–648

Strambini GB, Gabellieri E (1996) Proteins in frozen solutions: evidence of ice-induced partial unfolding. Biophys J 70:971–976

Strambini GB, Gonnelli M (1995) Tryptophan Phosphorescence in fluid solution. J Am Chem Soc 117:7646–7651

Strambini GB, Cioni P, Puntoni A (1989) Relationship between the conformation of glutamate dehydrogenase, the state of association of its subunit, and catalytic function. Biochemistry 28:3808–3814

Strambini GB, Kerwin BA, Mason BD, Gonnelli M (2004) The triplet-state lifetime of indole derivatives in aqueous solution. Photochem Photobiol 80:462–470

Tavares AJ, Chong LR, Petryayeva E, Algar WR, Krull UJ (2011) Quantum dots as contrast agents for in vivo tumor imaging: progress and issues. Anal Bioanal Chem 399:2331–2342

Thangadurai P, Balaji S, Manoharan PT (2008) Surface modification of CdS quantum dots using thiols—structural and photophysical studies. Nanotechnology 19:435708

Wu X, Liu H, Liu J, Haley KN, Treadway JA, Larson JP, Ge N, Peale F, Bruchez MP (2003) Immunofluorescent labeling of cancer marker Her2 and other cellular targets with semiconductor quantum dots. Nat Biotechnol 21:41–46

Yu WW, Qu LH, Guo WZ, Peng XG (2003) Experimental determination of the extinction coefficient of CdTe, CdSe, and CdS nanocrystals. Chem Mater 15:2854–2860

Zou L, Fang Z, Gu ZY, Zhong XH (2009) Aqueous phase synthesis of biostabilizer capped CdS nanocrystals with bright emission. J Lumin 129:536–540